ACS APPLIED MATERIALS & INTERFACES

Research Article

www.acsami.org

Conducting Hydrogels of Tetraaniline-g-poly(vinyl alcohol) in Situ Reinforced by Supramolecular Nanofibers

Huabo Huang,[†] Wan Li,[†] Hong Wang,*[,‡] Xiaoping Zeng,[†] Qin Wang,[‡] and Yajiang Yang*[,†,‡]

[†]Key Laboratory for Large-Format Battery Materials and Systems, Ministry of Education, and [‡]School of Chemistry and Chemical Engineering, Huazhong University of Science and Technology, Wuhan 430074, China

Supporting Information

ABSTRACT: Novel conducting hydrogels (PVA-TA) with dual network structures were synthesized by the grafting reaction of tetraaniline (TA) into the main chains of poly(vinyl alcohol) and in situ reinforced by self-assembly of a sorbitol derivative as the gelator. The chemical structure of the PVA-TA hydrogels was characterized by using FT-IR and NMR. The mechanical strength of the PVA-TA hydrogels was strongly improved due to the presence of supramolecular nanofibers. For instance, the compressive and tensile strengths of supramolecular nanofiber-reinforced hydrogels were, respectively, 10 times and 5 times higher than those of PVA-TA hydrogels. Their storage modulus (G′) and loss modulus (G″) were 5 times and 21 times higher than those of PVA-TA hydrogels, respectively. Cyclic voltammetry and conductivity measurements indicated that the electroactivity of reinforced hydrogels is not influenced by the presence of supramolecular nanofibers.

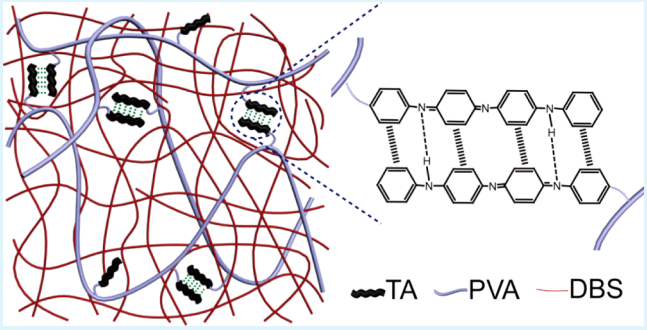

KEYWORDS: *supramolecular nanofibers, in situ reinforce, conducting hydrogels, tetraaniline, poly(vinyl alcohol)*

INTRODUCTION

Polymer hydrogels are typical soft materials and essentially water-swollen systems formed by polymerization of a hydrophilic monomer in the presence of a cross-linking agent.[1] Most polymer hydrogels possess the feature of environmental response, namely, responses of swelling and deswelling under an external stimulus, such as temperature, pH, light, and electric field, etc. Such unique features of polymer hydrogels endow a broad spectrum of applications in the fields of functional materials,[1] such as biomedical materials[2] and drug carriers.[3] In the developing trends of polymer hydrogels, it still remains a challenge to build in functionalities for novel applications and improving their mechanical strength.

In the field of polymer hydrogels, conducting hydrogels have received great attention in the past few years. We note that these so-called conducting polymer hydrogels are based on their intrinsic conducting polymers rather than on ionic compounds or other conducting species. Conducting polymer hydrogels are commonly prepared through the swelling of hydrogels in an acidic solution of monomers like aniline and followed by in situ polymerization.[4] The obtained conducting polymer hydrogels are essentially cross-linked polymers containing a semi-interpenetrating network structure. Alternatively, conducting polymer hydrogels can be also prepared by directly mixing aqueous solutions of aniline and poly(styrene sulfonate).[5] Other examples are chitosan-graft-polyaniline-based hydrogels[6] and pH-sensitive conducting polymer hydrogels.[7] These conducting polymer hydrogels have shown great potential applications in the fields of supercapacitors,[8] biological medicines,[9] conducting films,[10] and tissue-engineering materials.[11,12] However, these conducting polymer hydrogels suffer from phase separation and poor biocompatibility due to the high content of conducting polymers like polyaniline, polythiophene, or polypyrrole in the system.

Furthermore, a lack of mechanical strength is an inherent defect of polymer hydrogels.[13] Therefore, a large number of reports on the reinforcement of polymer hydrogels can be found in the literature. For example, the addition of various inorganic fillers, including nanofillers into the hydrogel matrices, is a common method to reinforce hydrogels.[14−17] The addition of another polymer to form a multi-interpenetrated network is also an effective method.[18,19] Also methods combining the addition of both inorganic fillers and multi-interpenetrated networks have been reported.[20] To a certain extent, these methods can improve the mechanical strength of hydrogels at the expense of environmental responsibility and biocompatibility. In order to overcome the limitations of the above methods, we made an attempt to endow hydrogel conductivity and at the same time improve the mechanical strength of hydrogels through the in situ reinforcement of supramolecular nanofibers. These nanofibers were formed by the noncovalent self-assembly of the gelator 1,3:2,4-

Received: October 8, 2013
Accepted: January 20, 2014
Published: January 20, 2014

   dx.doi.org/10.1021/am4043799 | ACS Appl. Mater. Interfaces 2014, 6, 1595−1600

di-*O*-benzylidene-D-sorbitol (DBS, sorbitol derivatives). As a typical small molecular gelator, DBS was widely investigated.[21,22] DBS can self-assemble in solvents via noncovalent interaction to form nanoscale entangled fibers and lead to the formation of supramolecular, three-dimensional network structures. Solvent molecules are immobilized by this supramolecular three-dimensional network structure, ultimately resulting in the formation of semisolid supramolecular organogels or hydrogels.[23,24]

In this work, we propose a new strategy to prepare conducting poly(vinyl alcohol) (PVA) hydrogels through the grafting reaction of tetraaniline (TA, also named aniline tetramer) onto the main chain of PVA and the noncovalent cross-linking between TA molecules. TA was employed here not only because of its good solubility in common solvents and its good biocompatibility but also because of its electroactivity like polyaniline.[25−28] Similarly, there are also reports on conducting hydrogels based on the coupling reaction between TA and an epoxy group[29] and chitosan.[30] PVA was employed here mainly due to its excellent biocompatibility. Furthermore, the conducting PVA-TA hydrogels were in situ reinforced by supramolecular nanofibers formed by the self-assembly of DBS. In other words, the solution of PVA-TA in DMSO/H_2O was solidified by DBS supramolecular structures. Our novel conducting hydrogels possess a dual-network structure of both a supramolecular network and a polymer network. It may find potential applications in the fields of biosensors and soft tissue engineering scaffolds.

EXPERIMENTAL SECTION

Materials. Poly(vinyl alcohol) (PVA, >99% hydrolyzed, average degree of polymerization 1750) was purchased from Sinopharm Chemical Reagent Co. 1,3:2,4-Di-*O*-benzylidene-D-sorbitol (DBS, purity 99.5%) was purchased from Wuhan Huabang Co. *N*-Phenyl-1,4-phenylenediamine (aniline dimer, purity 98%) was purchased from Aladdin Industrial Inc. and used as received. Dimethyl sulfoxide (DMSO) was purchased from Sinopharm Chemical Reagent Co. Before use, it was treated with CaH_2 at 70 °C and vacuum distilled, and then 4A molecular sieves were added to eliminate any remaining traces of water. Tolylene-2,4-diisocyanate (TDI) and dibutyl tin dilaurate (DBTDL) were purchased from Sinopharm Chemical Reagent Co. and used as received. All other chemicals and solvents were of analytical grade.

Synthesis of Tetraaniline (TA). TA was synthesized according to a method described elsewhere.[29,30] The detailed synthetic procedure can be found in the Supporting Information (SI).

Synthesis of Tetraaniline-Grafted Poly(vinyl alcohol) (PVA-TA). As shown in the synthetic route (SI, Scheme S1), 2.18 g of PVA was dissolved in 40 mL of DMSO. Subsequently 5 mL of toluene was used as an azeotropicic dehydration agent to eliminate any traces of water. In another flask, a solution of TA (0.36 g) and DMSO (15 mL) was added dropwise into a solution of TDI (0.17 g) in DMSO (10 mL) under the stirring. The solution mixture was left to react for 6 h at room temperature and then poured into the PVA solution. Subsequently, a few drops of DBTDL as catalyst were added into the mixture. The solution mixture was reacted at 75 °C for 5 h. The product (PVA-TA) was precipitated in ethanol, washed twice with acetone, and dried in vacuum at 40 °C for 24 h. The chemical structure of PVA-TA was characterized by FT-IR (SI, Figure S1) and ^{1}H NMR (SI, Figure S2).

Preparation of PVA-TA Hydrogels and Supramolecular Nanofiber-Reinforced PVA-TA Hydrogels. As shown in Table S1 (see SI), a designed amount of PVA-TA was dissolved in 1.5 mL of DMSO under heating and stirring. Subsequently 1.5 mL of deionized water was added until the solid was completely dissolved. The mixture was left for 24 h at room temperature to form a stable gel (SI, Figure S3). The gel samples were immersed in 0.1 mol/L aqueous solution of HCl for 8 h and then in a large amount of deionized water for 3 days to remove excess acid and DMSO. The deionized water was changed daily. After purification, the samples were fully swelled (saturated swelling). The water content in the hydrogels was approximately 89−93 wt %. The resultant hydrogels are denoted as PVA-TA-1, PVA-TA-2, and PVA-TA-3 according to the content of PVA-TA (SI, Table S1).

Similar to the above procedure, a designed amount of DBS was added into the solution of PVA-TA and DMSO. After purification, the samples were fully swelled. The water content in the hydrogels was approximately 91−94 wt %. The resultant PVA-TA/DBS hydrogels are denoted as PVA-TA/DBS-1, PVA-TA/DBS-2, and PVA-TA/DBS-3 (SI, Table S1), respectively.

UV−vis Spectroscopic Measurements. The UV−vis spectra of TA, PVA, and PVA-TA were recorded with a UV−vis spectrophotometer (TU-1810, Beijing Pushi General Co.) using DMSO as the solvent.

Field Emission Scanning Electron Microscopy (FE-SEM). PVA-TA and PVA-TA/DBS hydrogels were freeze-dried by liquid nitrogen and coated by gold for the FE-SEM measurements (Sirion 200, FEI). The accelerating voltage was 10 kV.

Measurement of Mechanical Properties. According to the method described elsewhere,[18,31] the mechanical properties of the hydrogels were measured with an electromechanical universal testing machine (CMT-4104, SANS) at room temperature. In the test of compression, cylindrical samples (φ18 × 8 mm) were placed between two plates. The compression speed was 1 mm/min. In the test of tensile, the hydrogels were cut into rectangular specimens (40 × 10 × 3 mm). The tensile speed was 5 mm/min.

Dynamic Rheological Measurements. The samples of the hydrogels were about 2 mm in thickness. Dynamic rheological measurements were performed on a rheometer (MCR 302, Anton Paar). The measurements were carried out with a shear strain amplitude of 0.1% in the frequency range from 1 to 100 rad/s at 25 °C.

Cyclic Voltammetry Measurements. The cyclic voltammetry measurements were conducted on an electrochemical workstation (IM6e, Zhanner) employing a three-electrode system with a platinum disk as working electrode, a platinum wire as auxiliary electrode, and a Ag/AgCl reference electrode. As a reference, a solution of TA/DMSO was coated onto the surface of the platinum plate electrode and dried into the film. The measurements were carried out in 1 mol/L aqueous solutions of HCl. The scan rate was 10 mV/s.

Conductivity Measurements. Samples of the hydrogels (0.5 × 0.5 × 0.5 cm) were sandwiched between two platinum plate electrodes to form a two-electrode system. The conductivities of the samples were determined from impedance spectra measured by an electrochemical workstation (CS330, Hust), and the data were treated by Zview software. The frequency was in the range of 0.01 Hz∼100 kHz, and the perturbation AC voltage was 10 mV. A three-component model was used for impedance analysis to deduce the bulk resistance R of the hydrogels.[32] The conductivity was calculated by the following equation

$$\sigma = \frac{1}{R}\frac{d}{S} \quad (1)$$

where σ is the conductivity; R is the resistance; and d and S are the thickness and area of the sample, respectively.

RESULTS AND DISCUSSION

Supramolecular Nanofiber-Reinforced PVA-TA Hydrogels. Unlike conventional polymer hydrogels, there is no cross-linker used in the formation of PVA-TA hydrogels because the cross-linked microdomains are formed by noncovalent interactions between TA molecules, such as hydrogen bonding and $\pi-\pi$ stacking[33] as shown in Figure 1. Furthermore, a large amount of water (∼90%)[18] contained inside the hydrogels leads to a poor mechanical strength. In this work, we use the

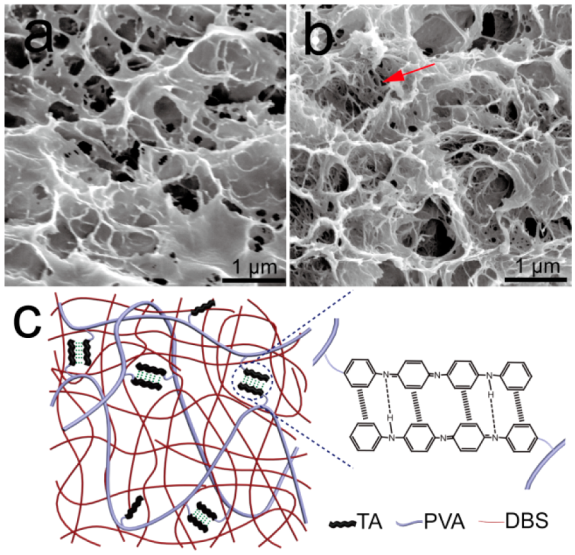

Figure 1. SEM images of a PVA-TA xerogel (a) and PVA-TA/DBS xerogel (b). A schematic illustration of supramolecular nanofiber-reinforced PVA-TA hydrogels is shown in (c).

supramolecular nanofibers formed by the self-assembly of sorbitol derivatives (DBS)[34] to prepare in situ reinforced PVA-TA hydrogels. Figure 1a shows the SEM image of the PVA-TA hydrogels without DBS nanofibers. Its microscopic morphology exhibits the typical porous structure of hydrogels. The pore size was found to be 0.3−1.5 μm. In the case of supramolecular nanofiber-reinforced PVA-TA hydrogels (Figure 1b), the pore structure was similar, but it now appears to consist of two interpenetrated networks. Therein, the thick and big network is most likely formed by the PVA-TA polymer. As indicated by the red arrow, the thin and small network is formed by the entangled DBS nanofibers. In our experiments, DBS was completely dissolved in the solution of PVA-TA and DMSO/water, resulting in a homogeneous solution. Thus, in the formation of the gels, DBS nanofibers were also homogeneously dispersed in the system. The size of the DBS nanofibers was found to be 20−80 nm, which can be calculated by the available software (ImageJ). The SEM image of PVA-TA with DBS nanofibers visually indicates that the hydrogels possess a dual interpenetrated network structure formed by a polymer network with a microscale size and a supramolecular network with a nanoscale size. Figure 1c schematically illustrates such dual interpenetrated network structures.

Figure 2 shows a diagram of the compressive stress/strain of the hydrogels. The compressive strengths of PVA-TA hydrogels without DBS nanofibers (curves 1−3) were lower than 0.3 MPa. Among them, the hydrogel containing more PVA-TA (curve 3) shows a relatively higher strength which can be attributed to the more cross-linked microdomains formed by TA. We note that the pure PVA cannot be a hydrogel under these conditions because no cross-linking microdomains are formed by TA. By contrast, the compressive strengths of the PVA-TA hydrogels with DBS nanofibers (curves 4−6) significantly increased to 0.9−3.1 MPa, about 10 times higher than that of the PVA-TA hydrogels without DBS nanofibers. Meanwhile, the elastic modulus of the PVA-TA hydrogels with DBS nanofibers can be calculated from the data of Figure 2.[35] For example, the elastic modulus of PVA-TA-3 was found to be 0.15 MPa. In the case of PVA-TA/DBS-3, it significantly increased to 0.72 MPa, also about 5 times higher than that

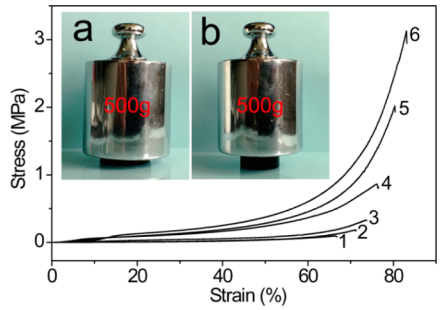

Figure 2. Diagram of compressive stress/strain of PVA-TA hydrogels and DBS nanofiber-reinforced hydrogels (PVA-TA/DBS). Curves 1−3 are PVA-TA-1, PVA-TA-2, and PVA-TA-3, respectively. Curves 4−6 are PVA-TA/DBS-1, PVA-TA/DBS-2, and PVA-TA-3, respectively. The inset optical photographs show the compression states of PVA-TA-3 (a) and PVA-TA/DBS-3 (b).

without DBS. The high elastic modulus implies that the materials possess excellent toughness. Apparently, such a reinforced effect should be attributed to the presence of a supramolecular network structure. The inset photographs in Figure 2 visually reflect the differences in strengths. Under the same weight press of 500 g, PVA-TA hydrogel became very thin, implying a poor compressive strength.

Figure 3 shows a diagram of the tensile stress/strain of the hydrogels. In comparison with the PVA-TA-3 hydrogel, the

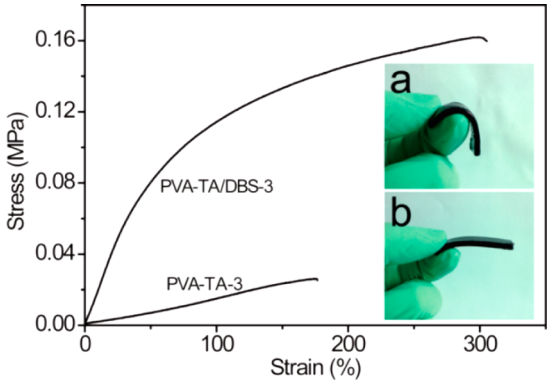

Figure 3. Diagram of the tensile stress/strain of PVA-TA-3 and PVA-TA/DBS-3 hydrogels. The inset optical photographs show the strength of PVA-TA-3 (a) and PVA-TA/DBS-3 (b).

tensile strength of the PVA-TA/DBS-3 hydrogel was significantly increased to 0.16 MPa, 5 times higher than that of the PVA-TA-3 hydrogel. Its breaking elongation also increased by 310%, 1.7 times higher than that of the PVA-TA-3 hydrogel. Also, the tensile elastic modulus of PVA-TA-3 was found to be 0.01 MPa. In the case of PVA-TA/DBS-3, it significantly increased to 0.19 MPa, almost 20 times higher than that without DBS. The inset photographs in Figure 3 show their differences in the mechanical properties. Supramolecular nanofiber-reinforced hydrogels show a satisfactory stiffness (inset photograph b). By contrast, a flexible state with almost no strength was found for the PVA-TA-3 hydrogel (inset photograph a). This is a significant result. In general, the micromechanic strength of noncovalent cross-linking microdomains formed by TA is relatively weak. These microdomains easily become the sites of stress concentration under the effect of external forces, ultimately resulting in destruction of the materials. The supramolecular network interpenetrated within

dx.doi.org/10.1021/am4043799 | ACS Appl. Mater. Interfaces 2014, 6, 1595−1600

the PVA-TA network may play a role in the dissipation of stress around the noncovalent cross-linking microdomains. Therefore, the supramolecular network can prevent the tendency to grow from a microscopic destruction to a macroscopic destruction. This may be a reason why a supramolecular network can reinforce the PVA-TA hydrogels. We note that a significant difference of strength between the gels with and without DBS was found when 2 wt % of DBS was applied. Thus, all samples were prepared by using 2 wt % of DBS in this work.

The above discussion is based on a consideration of static mechanical properties. Since the relaxation process of the polymer is sensitive to the frequency of external forces, we measured dynamic viscoelastic spectra of the hydrogels (Figure 4). In the range of the test frequencies, the storage modulus

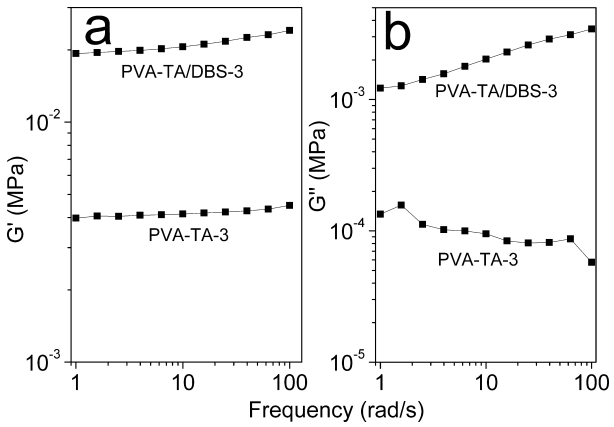

Figure 4. Rheological determination of the storage modulus (G′, plot a) and loss modulus (G″, plot b) as a function of frequency for PVA-TA/DBS-3 and PVA-TA-3 hydrogels.

(G′) and loss modulus (G″) of the supramolecular nanofiber-reinforced hydrogels were higher than those of the PVA-TA hydrogels. For instance, at a frequency of 10 rad/s, the G′ and G″ of PVA-TA-3 were found to be only 4×10^{-3} and 9×10^{-5} MPa, respectively. Contrastingly, the G′ and G″ of PVA-TA/DBS-3 were 2×10^{-2} and 2×10^{-3} MPa, respectively, 5 times and 21 times higher than those of the former. In general, the dynamic storage modulus is the most important parameter to assess the deformation capability of materials. In other words, it represents the characterization of the stiffness of materials. Apparently, the PVA-TA/DBS-3 hydrogels show a better ability to resist deformation as a result of external forces. This can be attributed to their dual-network structure resulting from supramolecular and polymer networks within the hydrogels as observed in the SEM images (Figure 1). The loss modulus (G″) characterizes the damping property of materials. In general, the higher the value of G″, the higher the toughness of materials is. It was also found that the loss modulus of PVA-TA-3 decreased with an increase of the frequency. It may be attributed to the relatively weak micromechanical strength of noncovalent cross-linking microdomains formed by TA. Under the circumstances of high shear frequencies and the absence of support by nanofibers, such physical cross-linking could be easily damaged. The results in Figure 4 indicate that DBS supramolecular nanofibers not only improve the ability to resist deformation but also are beneficial to increase the ability of break resistance.

Electroactivity of Supramolecular Nanofiber-Reinforced PVA-TA Hydrogels. TA molecules possess electroactivity due to their conjugated structure. To estimate whether TA is still electroactive after the grafting reaction on the PVA main chains, we first measured the UV−vis spectra of the PVA-TA hydrogels (Figure 5). The pure TA shows two distinct

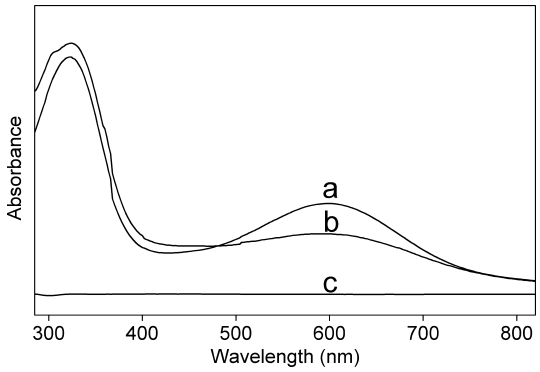

Figure 5. UV−vis spectra of TA (a), PVA-TA (b), and PVA (c).

absorption peaks at 320 and 600 nm (spectrum a). They are assigned to the $\pi-\pi^*$ transition of the benzene ring and the benzenoid to quiniod ($\pi_B-\pi_Q$) excitonic transition.[33] As a reference, the PVA without TA does not show any absorption peak in the range of the test wavelengths (spectrum c). In the case of PVA-TA, two absorption peaks at the same positions can be observed, but the peak intensity ratios of 600−320 nm were found to be somewhat less than that of pure TA. This may be ascribed to the effect of neighboring groups on the grafted TA,[30,33] like electron-withdrawing interaction due to the TDI species. Additionally, the shape of the absorption peaks was similar to that of pure TA. These results indicate that TA retains about the same electroactivity after the grafting reaction.

Figure 6 shows cyclic voltammetric measurements of TA, PVA-TA, and PVA-TA/DBS hydrogels. Herein, pure TA shows two distinct peaks of oxidation at 0.40 and 0.57 V (Figure 6a), which can be assigned to the transition from a leucoemeraldine base state to an emeraldine state and a further transition to a pernigraniline state.[26,33] PVA-TA hydrogels show three peaks of oxidation at −0.15, 0.31, and 0.56 V (blue curve in Figure 6b). By contrast, however, the intensities of the peak currents were lower than that of pure TA. The reason may involve the weak signal due to the low content of TA within the hydrogels. Another reason may involve the influence of neighboring groups, such as the acylamino groups of TDI, leading to a change of the electrochemical redox process. Nevertheless, the peak potentials and peak currents of PVA-TA/DBS were found to be rather similar to that of PVA-TA (red curve in Figure 6b). As a consequence, it is likely that the introduction of DBS supramolecular nanofibers does not influence the electrochemical redox process as well as the ability of charge transfer within PVA-TA hydrogels.

Figure 7 shows conductivities of the PVA-TA/DBS and PVA-TA hydrogels. In general, PVA is a nonconductive polymer. We note that there are no ions incorporated in the hydrogels. Therefore, the conductivity of the PVA-TA hydrogels should be attributed to electron transfer of TA and depending on the content of the TA species. In general, the higher the content of PVA-TA, the higher the conductivity is. As in the case of PVA-TA-3, a high content of PVA-TA makes it easier to form the conductive network structure. As shown in Figure 7, the conductivities of PVA-TA/DBS hydrogels seem to be little less than those of the PVA-TA hydrogels, but they have

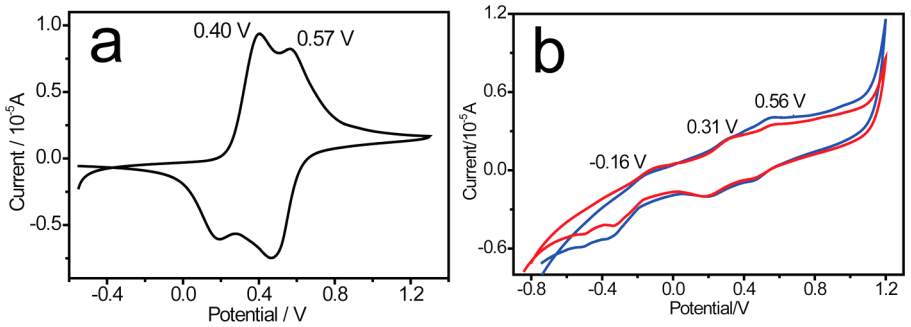

Figure 6. Cyclic voltammetry of TA (a), PVA-TA (blue curve in plot b), and PVA-TA/DBS (red curve in plot b).

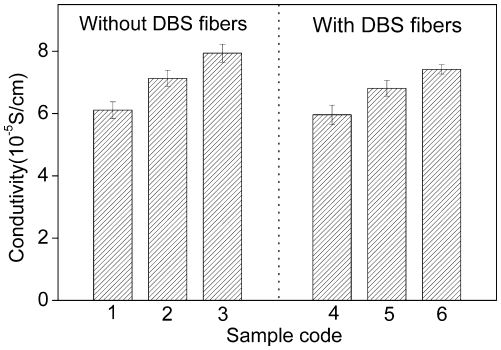

Figure 7. Conductivity of PVA-TA hydrogels without/with DBS supramolecular nanofibers. The columns of 1−3 represent PVA-TA-1, PVA-TA-2, and PVA-TA-3 hydrogels, respectively. The columns of 4−6 represent the corresponding hydrogels with DBS supramolecular nanofibers.

the same order of magnitude (10^{-5} S/cm). In general, more TA species in the system are beneficial to increase conductivity. In our experiments, however, it was found that more TA may cause a nonuniform structure of the system. Although the conductivity of the resultant hydrogels is relatively low due to the limitation of the intrinsic conductive ability of TA, the supramolecular nanofiber-reinforced PVA-TA hydrogels can be expected to possess a potential for application in the fields of biomaterials and biosensors.[36] For instance, these conductivity values are adequate to transfer bioelectrical signals in vivo and electrical stimulation on the cell proliferation and differentiation because the microcurrent intensity in the human body is quite low.[29,30]

CONCLUSIONS

In this work, we propose a new strategy for the preparation of conducting hydrogels reinforced by supramolecular nanofibers. Electroactive tetraaniline (TA) was grafted on the main chains of PVA via reaction with tolylene-2,4-diisocyanate. On the basis of the noncovalent interaction between TA molecules, the resulting conducting PVA-TA hydrogels were formed without any external addition of cross-linker and conducting species. The hydrogels show poor mechanical properties, but this can be improved by in situ supramolecular self-assembly of a sorbitol gelator within the hydrogels. The reinforcing mechanism is ascribed to the formation of a dual-network structure. The introduction of the supramolecular nanofibers does not influence the electrical properties of the hydrogels. The reinforced hydrogels may well have potential applications in the fields of biosensors and scaffold materials for soft tissue engineering.

ASSOCIATED CONTENT

Supporting Information

The synthesis and structural characterization of tetraaniline and tetraaniline-grafted PVA. This material is available free of charge via the Internet at http://pubs.acs.org.

AUTHOR INFORMATION

Corresponding Author

*E-mail: yjyang@mail.hust.edu.cn. Tel.: +862787547141. Fax: +862787543632.

Notes

The authors declare no competing financial interest.

ACKNOWLEDGMENTS

The work was financially supported by the National Basic Research Program of China (2012CB932500) and the National Natural Science Foundation of China (51073062). We also thank the HUST Analytical and Testing Center for the SEM measurements.

REFERENCES

(1) Sahu, N. K.; Gils, P. S.; Ray, D.; Sahoo, P. K. *Adv. Polym. Sci. Technol. Int. J.* **2012**, *2*, 43−50.
(2) Hoffman, A. S. *Adv. Drug Deliver. Rev.* **2012**, *64*, 18−23.
(3) Wang, Q.; Xu, H.; Yang, X.; Yang, Y. *Int. J. Pharmaceut.* **2008**, *361*, 189−193.
(4) Molina, M. A.; Rivarola, C. R.; Barbero, C. A. *Eur. Polym. J.* **2011**, *47*, 1977−1984.
(5) Dai, T.; Jia, Y. *Polymer* **2011**, *52*, 2550−2558.
(6) Marcasuzaa, P.; Reynaud, S.; Ehrenfeld, F.; Khoukh, A.; Desbrieres, J. *Biomacromolecules* **2010**, *11*, 1684−1691.
(7) Naficy, S.; Razal, J. M.; Spinks, G. M.; Wallace, G. G.; Whitten, P. G. *Chem. Mater.* **2012**, *24*, 3425−3433.
(8) Ghosh, S.; Inganäs, O. *Adv. Mater.* **1999**, *11*, 1214−1218.
(9) Green, R. A.; Baek, S.; Poole-Warren, L. A.; Martens, P. J. *Sci. Technol. Adv. Mater.* **2010**, *11*, 014107.
(10) Jin, L.; Zhao, Y. J.; Liu, X.; Wang, Y. L.; Ye, B. F.; Xie, Z. Y.; Gu, Z. Z. *Soft Matter* **2012**, *8*, 4911−4917.
(11) Mawad, D.; Stewart, E.; Officer, D. L.; Romeo, T.; Wagner, P.; Wagner, K.; Wallace, G. G. *Adv. Funct. Mater.* **2012**, *22*, 2692−2699.
(12) Guiseppi-Elie, A. *Biomaterials* **2010**, *31*, 2701−2716.
(13) Haque, Md. A.; Kurokawa, T.; Gong, J. P. *Polymer* **2012**, *53*, 1805−1822.
(14) Shikinaka, K.; Koizumi, Y.; Osada, Y.; Shigehara, K. *Polym. Advan. Technol.* **2011**, *22*, 1212−1215.
(15) Liu, M. X.; Li, W. D.; Rong, J. H.; Zhou, C. R. *Colloid Polym. Sci.* **2012**, *290*, 895−905.
(16) Abitbol, T.; Johnstone, T.; Quinn, T. M.; Gray, D. G. *Soft Matter* **2011**, *7*, 2373−2379.
(17) Song, H.; Luo, Z.; Zhao, H.; Luo, S.; Wu, X.; Gao, J.; Wang, Z. *RSC Adv.* **2013**, *3*, 11665−11675.

(18) Dai, T.; Qing, X.; Lu, Y.; Xia, Y. *Polymer* **2009**, *50*, 5236−5241.
(19) Tang, Q. W.; Sun, X. M.; Li, Q. H.; Wu, J. H.; Lin, J. M. *Colloid. Surface A* **2009**, *346*, 91−98.
(20) Wang, Q.; Hou, R.; Cheng, Y.; Fu, J. *Soft Matter* **2012**, *8*, 6048−6056.
(21) Jin, L.; Wang, H.; Yang, Y. *Compos. Sci. Technol.* **2013**, *79*, 58−63.
(22) Chen, W. Y.; Yang, Y. J.; Lee, C. H.; Shen, A. Q. *Langmuir* **2008**, *24*, 10432−10436.
(23) George, M.; Weiss, R. G. *Acc. Chem. Res.* **2006**, *39*, 489−497.
(24) Sangeetha, N. M.; Maitra, U. *Chem. Soc. Rev.* **2005**, *34*, 821−836.
(25) Rozalska, I.; Kulyk, P.; Kulszewicz-Bajer, I. *New J. Chem.* **2004**, *28*, 1235−1243.
(26) Chen, L.; Yu, Y.; Mao, H.; Lu, X.; Zhang, W.; Wei, Y. *Mater. Lett.* **2005**, *59*, 2446−2450.
(27) Guo, B.; Finne-Wistrand, A.; Albertsson, A.-C. *Macromolecules* **2011**, *45*, 652−659.
(28) Ford, W. E.; Gao, D.; Scholz, F.; Nelles, G.; von Wrochem, F. *ACS Nano* **2013**, *7*, 1943−1951.
(29) Guo, B. L.; Finne-Wistrand, A.; Albertsson, A. C. *Chem. Mater.* **2011**, *23*, 1254−1262.
(30) Guo, B.; Finne-Wistrand, A.; Albertsson, A. C. *Biomacromolecules* **2011**, *12*, 2601−2609.
(31) Zhang, J.; Wang, N.; Liu, W.; Zhao, X.; Lu, W. *Soft Matter* **2013**, *9*, 6331−6337.
(32) Saha, S.; Schön, E.-M.; Cativiela, C.; Díaz, D. D; Banerjee, R. *Chem.—Eur. J.* **2013**, *19*, 9562−9568.
(33) Yang, Z.; Wang, X.; Yang, Y.; Liao, Y.; Wei, Y.; Xie, X. *Langmuir* **2010**, *26*, 9386−9392.
(34) Wang, H.; Yi, C.; Li, X.; Fang, F.; Yang, Y. *J. Lumin.* **2011**, *131*, 603−607.
(35) He, C.; Jiao, K.; Zhang, X.; Xiang, M.; Li, Z.; Wang, H. *Soft Matter* **2011**, *7*, 2943−2952.
(36) Niple, J. C.; Daigle, J. P.; Zaffanella, L. E.; Sullivan, T.; Kavet, R. *Bioelectromagnetics* **2004**, *25*, 369−373.